Plant Cell Rep (2014) 33:1829–1841
DOI 10.1007/s00299-014-1660-1

ORIGINAL PAPER

Overexpression of *Camellia sinensis* H1 histone gene confers abiotic stress tolerance in transgenic tobacco

Weidong Wang · Yuhua Wang · Yulin Du · Zhen Zhao · Xujun Zhu · Xin Jiang · Zaifa Shu · Ying Yin · Xinghui Li

Received: 6 May 2014 / Revised: 7 July 2014 / Accepted: 14 July 2014 / Published online: 26 July 2014

Abstract

Key message **Overexpression of *CsHis* in tobacco promoted chromatin condensation, but did not affect the phenotype. It also conferred tolerance to low-temperature, high-salinity, ABA, drought and oxidative stress in transgenic tobacco.**

Abstract H1 histone, as a major structural protein of higher-order chromatin, is associated with stress responses in plants. Here, we describe the functions of the *Camellia sinensis* H1 Histone gene (*CsHis*) to illustrate its roles in plant responses to stresses. Subcellular localization and prokaryotic expression assays showed that the CsHis protein is localized in the nucleus, and its molecular size is approximately 22.5 kD. The expression levels of *CsHis* in *C. sinensis* leaves under various conditions were investigated by qRT-PCR, and the results indicated that *CsHis* was strongly induced by various abiotic stresses such as low-temperature, high-salinity, ABA, drought and oxidative stress. Overexpression of *CsHis* in tobacco (*Nicotiana tabacum*) promoted chromatin condensation, while there were almost no changes in the growth and development of transgenic tobacco plants. Phylogenetic analysis showed that CsHis belongs to the H1C and H1D variants of H1 histones, which are stress-induced variants and not the key variants required for growth and development. Stress tolerance analysis indicated that the transgenic tobacco plants exhibited higher tolerance than the WT plants upon exposure to various abiotic stresses; the transgenic plants displayed reduced wilting and senescence and exhibited greater net photosynthetic rate (Pn), stomatal conductance (Gs) and maximal photochemical efficiency (Fv/Fm) values. All the above results suggest that *CsHis* is a stress-induced gene and that its overexpression improves the tolerance to various abiotic stresses in the transgenic tobacco plants, possibly through the maintenance of photosynthetic efficiency.

Keywords Abiotic stress tolerance · *Camellia sinensis* · H1 histone · Transgenic tobacco

Communicated by Prakash Lakshmanan.

W. Wang and Y. Wang these authors contributed equally to this work.

Electronic supplementary material The online version of this article (doi:10.1007/s00299-014-1660-1) contains supplementary material, which is available to authorized users.

W. Wang · Y. Wang · Y. Du · Z. Zhao · X. Zhu · X. Jiang · Z. Shu · Y. Yin · X. Li (✉)
Tea Science Research Institute, Nanjing Agricultural University, Nanjing 210095, China
e-mail: lxh@njau.edu.cn

W. Wang
e-mail: 2013204029@njau.edu.cn

Y. Wang
e-mail: wangyuhua@njau.edu.cn

Y. Du
e-mail: 2012104094@njau.edu.cn

Z. Zhao
e-mail: zhenzhenyu1989@163.com

X. Zhu
e-mail: zhuxujun@njau.edu.cn

X. Jiang
e-mail: jiang0xin@126.com

Z. Shu
e-mail: 2013104093@njau.edu.cn

Y. Yin
e-mail: yinying0106@126.com

Abbreviations

ABA	Abscisic acid
CaMV	*Cauliflower mosaic* virus
Fv/Fm	Maximal photochemical efficiency
GFP	Green fluorescent protein
Gs	Stomatal conductance
ORF	Open reading frame
PEG 6000	Polyethylene glycol 6000
Pn	Net photosynthetic rate
qRT-PCR	Quantitative real-time PCR
PCR	Polymerase chain reaction
RT-PCR	Reverse transcription polymerase chain reaction
WT	Wild type

Introduction

In eukaryotic cells, the complex structural organization of chromatin regulates gene expression, which is critical during the life cycle (Kornberg and Lorch 1999). The fundamental repeating unit of chromatin is the nucleosome, which is comprised of approximately 147 bp of DNA wrapped around a core histone octamer. Each octamer consists of two copies of core histone, H2A, H2B, H3 and H4 (Raghuram et al. 2009). Additionally, the nucleosomes are connected by stretches of 'linker DNA' and compacted by a linker histone known as H1 histone. Furthermore, H1 histone is a lysine-rich nucleoprotein that stabilizes and enhances the folding of nucleosomal threads into 30-nm fibers (Widom 1998). Thus, this histone plays important roles in the generation of higher-order chromatin structure. According to previous reports, the roles of core histones in regulating chromatin structure and gene expression are relatively well understood (Kornberg and Lorch 1999; Wierzbicki and Jerzmanowski 2005), while little is known about the biological functions of H1 histone.

Previous studies showed that H1 histone plays a key role in the general repression of gene expression as a structural protein of chromatin (Laybourn and Kadonaga 1991). However, accumulating evidence has shown that the model of H1 histone as a general transcriptional suppressor was oversimplified (Raghuram et al. 2009; Wolffe et al. 1997). For example, Shen and Gorovsky (1996) demonstrated that H1 histone was a key factor in activating the expression of the *CyP* (Cysteine protease) gene in *Tetrahymena* cells, suggesting that H1 histone is crucial to many life processes including development, differentiation, apoptosis, aging and senescence (Raghuram et al. 2009; Wolffe et al. 1997). Moreover, the *H1 histone* genes from several plant species such as *Arabidopsis thaliana* (Ascenzi and Gantt 1997), maize (Razafimahatratra et al. 1991), wheat (Yang et al. 1991), tomato (Jayawardene and Riggs 1994), tobacco (Szekeres et al. 1995), banana (Wang et al. 2012a), and cotton (Trivedi et al. 2012) have been cloned and sequenced. Furthermore, different variants of H1 histone were distinguished according to their structures and functions, including H1A, H1B, H1C, H1D, H1E and H1F. The two major variants, H1A and H1B, account for more than 80 % of chromatin linker histones and are involved in vegetative growth, tissue differentiation, male meiosis and pollen germination in plants. Two of the minor variants, H1C and H1D, were provisionally characterized as stress-inducible proteins, but their roles in plants remain unclear (Prymakowska-Bosak et al. 1999; Przewloka et al. 2002). Some findings have confirmed that *H1 histone* is a stress-induced gene in plants (Ascenzi and Gantt 1997; Kreps et al. 2002; Scippa et al. 2000; Wei and O'Connell 1996). For example, Wang et al. (2012a) reported that the expression level of *H1 histone* was significantly increased by stress treatments and exogenous hormone treatment in banana fruit, while Trivedi et al. (2012) reported the accumulation of an H1 histone variant during epigenetic regulation of drought tolerance in *Gossypium herbaceum*. However, the mechanism underlying the involvement of H1 histone in stress response and in conferring stress tolerance in plants is still unknown.

Tea [*Camellia sinensis* (L.) O. Kuntze] is a perennial evergreen woody crop grown in different agro-climatic zones. The plant has to cope with various abiotic stresses during its lifecycle, such as drought stress (Das et al. 2012), salinity stress (Li et al. 2010), heavy-metal stress (Basak et al. 2001), and especially cold stress, which is a major factor that significantly constrains the geographical distribution of *C. sinensis* and ultimately affects the economic benefits of tea production (Li et al. 2010, Wang et al. 2012b). In our previous study, *H1 histone* of *C. sinensis* (*CsHis*, GenBank Accession No. EU716314) was isolated and identified by cDNA-AFLP. Moreover, promoter analysis indicated that the promoter of the *CsHis* gene contained several *cis*-acting enhancer elements important for abscisic acid (ABA) and stress responsiveness, such as ABRE, ARE and TC-rich repeats, implying that the *CsHis* gene may be strongly induced by ABA and stress treatments (Fang et al. 2013). However, whether CsHis is directly involved in stress response and tolerance in *C. sinensis* remains unknown. In the present study, we investigated the subcellular localization of the CsHis protein and the expression levels of *CsHis* in *C. sinensis* leaves under various abiotic stresses, including low-temperature, high-salinity, ABA, drought and oxidative stress. Additionally, transgenic tobacco plants overexpressing *CsHis* were obtained, and ultrastructure observation and abiotic stress tolerance analyses were performed to explore the roles of CsHis during abiotic stresses.

Materials and methods

Plant materials, growth conditions, and abiotic stress treatments

Two-year-old tea plants of the cultivar '*Camellia sinensis* (L.) O. Kuntze cv. *Yingshuang*' (a cultivar of *C. sinensis* with good stress tolerance) were pre-incubated in control nutrient solution (Wan et al. 2012) at 25 ± 1 °C for 2 weeks in an artificial climate chamber under a 16-h light (240 μmol m^{-2} s^{-1})/8-h dark cycle. Then, some of the pre-incubated plants were transferred to another artificial climate chamber and maintained at 4 °C for low-temperature treatment. For abiotic stress assays, different nutrient solutions containing 600-mM NaCl, 50-μM abscisic acid (ABA), 20 % w/v polyethylene glycol (PEG) 6000 or 100-mM H_2O_2 were used. The fourth leaves from the top of the *C. sinensis* plants were collected after incubating the plants for 0, 1, 4, 8, 12 and 24 h under control or stress conditions, and the samples were immediately frozen in liquid nitrogen and stored at −70 °C until use.

Isolation and cloning of the *CsHis* gene

Total RNA was extracted from *C. sinensis* leaves with RNAiso Plus (TaKaRa, Japan) following the manufacturer's instructions, and the RNA was reverse transcribed to cDNA using the PrimeScript™ 1st Strand cDNA Synthesis Kit (TaKaRa, Dalian, China) according to the manufacturer's instructions. To isolate *CsHis*, cDNA and primers (CsHis-ORF-F and -R, Table S1) designed based on the sequence of the ORF from GenBank (Accession No. EU716314) were used for polymerase chain reaction (PCR) amplification, and the products were cloned into the pMD®18-T Vector (TaKaRa, Dalian, China) for sequencing (GenScript, China).

Subcellular localization of the CsHis protein

To construct the CsHis::GFP vector, the *CsHis* ORF was amplified by PCR using CsHis-SL-F and -R (Table S1) as primers, and then, the PCR product was cloned into the pJIT166-GFP vector upstream of the green fluorescent protein (GFP) sequence. Subsequently, the *CsHis::GFP* fusion and *GFP* alone vectors were transiently introduced into onion (*Allium cepa*) epidermal cells by a Biolistic Transformation System (PDS-1000/He, Bio-Rad, USA). Tissues were incubated for 16 h at 25 °C in the dark after bombardment. A fluorescence assay was performed on a Laser Scanning Confocal Microscope (LSCM, TCS SP2, Leica, Germany). Gray images were captured for each color channel and then merged using the Leica LCS software.

Prokaryotic expression and Western blotting of CsHis protein

CsHis-PE-F and -R (Table S1) were used as primers to amplify the *CsHis* ORF, and the PCR product was cloned into the pET-32a(+) vector upstream of the Trx-tag. Then, validated pET-32a(+)-CsHis plasmids and the pET-32a(+) empty vector were transfected into competent BL21(DE3) *E. coli* cells following the method of Sambrook and Russell (2001). The fusion protein was expressed according to the methods described by Li et al. (2012). Furthermore, the fusion protein was collected and analyzed by 12 % sodium dodecyl sulfate polyacrylamide gel electrophoresis (SDS–PAGE). After electrophoresis, the gel was stained with Coomassie brilliant blue and photographed. Western blotting analysis was carried out as Fu et al. (2011) described with small modifications. Briefly, separated proteins were transferred to polyvinylidene difluoride (PVDF) membranes using a semi-dry transfer system. Then, the membrane was rinsed with phosphate-buffered saline (PBS, pH 7.4) and incubated for 2 h at room temperature in blocking solution (PBS containing 5 % skim milk). Membranes were subsequently incubated for 1 h at 37 °C with primary antibody (mouse anti-Trx-tag monoclonal antibody) diluted 1:1,000 in blocking solution. Finally, immune complexes were detected using horseradish peroxidase (HRP)-conjugated goat anti-mouse IgG by electro-chemiluminescence (ECL) in the dark.

Quantitative real-time PCR (qRT-PCR)

Total RNA from leaves was extracted using RNAiso Plus (TaKaRa, Japan) and treated with DNase to remove any genomic DNA contamination. The quality of total RNA was measured with the ONE DropTM OD-1000+ spectrophotometer (ONE Drop, USA), and the RNA was reverse transcribed to cDNA using the PrimeScript™ 1st Strand cDNA Synthesis Kit (TaKaRa, Dalian, China). The qRT-PCR was carried out using SYBR® *Premix Ex Taq*™ II (TaKaRa, Dalian, China) on an IQ5 Multicolor Real-Time PCR Detection System (Bio-Rad, Hercules, CA, USA) according to the manufacturer's instructions. Briefly, the amplification regimen consisted of an initial denaturation at 95 °C for 30 s, followed by 40 cycles of 95 °C for 5 s and 60 °C for 30 s. *C. sinensis CsGAPDH* (cytosolic glyceraldehyde-3-phosphate dehydrogenase, unpublished) was amplified as an internal control. Primers used for qRT-PCR are listed in Table S1. Relative expression levels were calculated by the $2^{-\Delta\Delta CT}$ method, where ΔΔCT = (CT, Target-CT, GAPDH) $Time_x$-(CT, Target-CT, GAPDH) $Time_0$ (Livak and Schmittgen 2001). Values represent the average of three technical replicates.

Construction of plant expression vectors and tobacco transformation

The *CsHis* ORF was amplified with the CsHis-F/-R primer pair (Table S1) and harbored a 5′ *Kpn* I restriction site and a 3′ *BamH* I restriction site. The amplicon digested by *Kpn* I and *BamH* I was inserted into the plant expression vector pCAMBIA2300 (produced for C-terminal protein fusions with GFP) under the control of the cauliflower mosaic virus (CaMV) 35S promoter to generate a *35S::CsHis::GFP* construct. Then, the recombinant plasmids were introduced into *Agrobacterium tumefaciens* strain GV3101 and transformed into tobacco plants by the leaf disc method (Voelker et al. 1987). The transgenic tobacco plants were screened using 50-mg L^{-1} kanamycin, and transformation was confirmed by fluorescence observation with a stereomicroscope (MVX10, OLYMPUS, Japan) as well as PCR and RT-PCR with primers CsHis-ORF-F and -R (Table S1). Only those plants containing and expressing the *CsHis* gene were used for further analysis.

Ultrastructure observation with a transmission electron microscope (TEM)

Ultrastructural changes were studied by observing ultrathin sections of leaves according to Huang et al. (2009) with slight modification. In brief, 1.5 × 2 mm^2 samples were cut from leaves (at exactly the same stage) of the transgenic and wild-type (WT) tobacco plants, and then, they were fixed in 2.5 % glutaraldehyde in 0.1 M phosphate buffer solution (PBS, pH 7.2) at 4 °C for 4 h, followed by 2-h post-fixation in 1 % OsO_4 at room temperature. The samples were subsequently dehydrated with an ethanol gradient (50, 70, 90 and 100 %) and embedded with Epon812 epoxy resin and acetone. Finally, the samples were cut ultrathin by a Power-Tome-XL Ultramicrotome (RMC, USA), and the ultrathin sections were stained with uranyl acetate and lead citrate for ultrastructure observation using a TEM (H-7650, Hitachi High-technologies Corporation, Japan).

Physiological analysis of transgenic plants and abiotic stress tolerance

Leaf disc assay

Transgenic and WT tobacco plants were grown in 1/2 Hoagland's nutrient solution at 25 ± 1 °C in an artificial climate chamber under a 16-h light (240 μmol m^{-2} s^{-1})/8-h dark cycle. The leaf discs (2.5 cm^2) were cut from healthy and fully expanded leaves of 8-week-old transgenic and WT tobacco plants and incubated for 5 days at 25 ± 1 °C in 15-mL distilled water as the control or in solutions containing NaCl (600 mM), ABA (50 μM), PEG 6000 (20 %) or H_2O_2 (100 mM) as the stress treatments; low-temperature treatment was performed with distilled water at 4 °C. All leaf discs were incubated under a continuous white light intensity of 120 μmol m^{-2} s^{-1}. Phenotypic changes and chlorophyll content were measured to detect the effects of various treatments on leaf discs according to Liu et al. (2013) and Alsaadawi et al. (1986), respectively.

Measurements of photosynthetic gas exchange and chlorophyll fluorescence parameters

Twelve-week-old and growth vigor-consistent transgenic and WT tobacco plants were exposed to low temperature (4 °C), NaCl (600 mM), ABA (50 μM), PEG 6000 (20 %) or H_2O_2 (100 mM) for 3 days. Photosynthetic gas exchange measurements were taken on randomly selected and fully expanded leaves using a Portable Photosynthesis System (LI-6400XT, Li-Cor Inc., Neb., USA) in an open system. Net photosynthetic rate (Pn) and stomatal conductance to CO_2 (Gs) were determined at an ambient CO_2 concentration of 380 ± 10 ppm, a temperature of 25 ± 1 °C, 50 ± 5 % relative humidity and a photon flux density of 1,000 μmol m^{-2} s^{-1}. Simultaneously, the leaf discs (7.0 cm^2) were cut from randomly selected and fully expanded leaves of the transgenic and WT tobacco plants using a cork borer. Then, the chlorophyll fluorescence parameters of leaf discs were measured using an Imaging-PAM Chlorophyll Fluorometer (M-series, Heinz Walz GmbH, Germany) at room temperature (25 °C). All the tobacco plants were dark-adapted for 30 min before the measurement was carried out according to the method described by Gao et al. (2012). The maximal photochemical efficiency (Fv/Fm) was calculated automatically.

Statistical analyses

All data are expressed as the arithmetic mean ± standard deviations (SD) obtained from at least three independent replicates. Statistical significance was calculated by one-way ANOVA using Tukey's test, and the significant differences among various treatment groups are represented by '*' at $P < 0.05$ and '**' at $P < 0.01$. Analyses were performed with the IBM SPSS Statistics 20 software.

Results

Subcellular localization of the CsHis protein

CsHis was predicted to be localized in nuclei by WoLF PSORT (http://wolfpsort.org) and TargetP (http://genome.

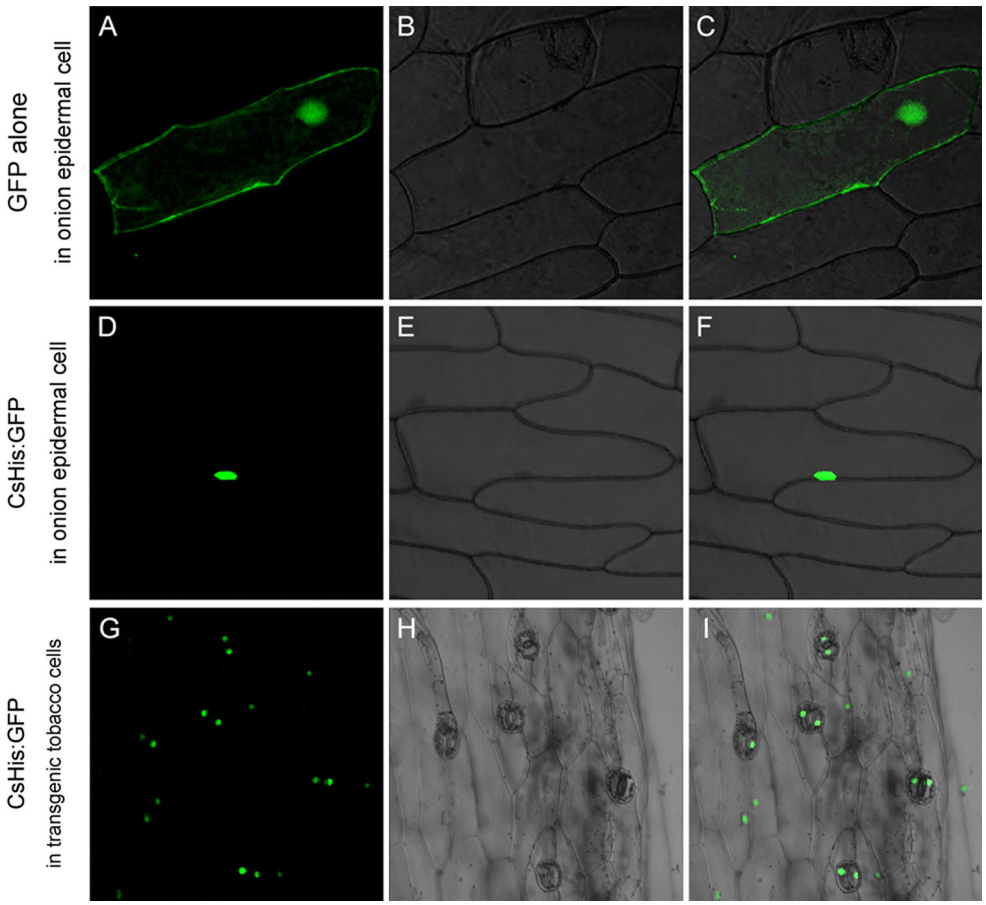

Fig. 1 Subcellular localization of the CsHis protein in an onion epidermal cell and transgenic tobacco cells. An onion epidermal cell expressing GFP alone (**a**); the DIC image (**b**) and the merged image (**c**) show *green* fluorescent signals in the nucleus, the plasma membrane and the cytoplasm. An onion epidermal cell expressing the CsHis::GFP fusion (**d**); the DIC image (**e**) and the merged image (**f**) show *green* fluorescent signals only in the nucleus. Transgenic tobacco cells expressing the CsHis::GFP fusion (**g**); the DIC image (**h**) and the merged image (**i**) show *green* fluorescence only in the nucleus (color figure online)

cbs.dtu.dk/services/TargetP/). To validate the prediction, *CsHis::GFP* (green fluorescent protein) fusion genes under the control of a double CaMV 35S promoter (Fig. S1A) were transfected into onion (*Allium cepa*) epidermal cells. Meanwhile, the *GFP* gene alone was transfected as a control. As shown in Fig. 1a–c, the green fluorescent signals of the GFP control was observed in all regions of the onion epidermal cell, including the nucleus, the plasma membrane and the cytoplasm, whereas the green fluorescence of the CsHis::GFP fusion was observed only in the nucleus (Fig. 1d–f). Additionally, the green fluorescence of the CsHis::GFP fusion also occurred in the nuclei of transgenic tobacco cells (Fig. 1g, h), implying that the CsHis protein is a nucleus-localized protein.

Expression of the TrX::CsHis fusion protein

The TrX::CsHis fusion expression vector was constructed (Fig. S1B) and transfected into competent BL21 (DE3) *E. coli* cell. In an SDS–PAGE assay (Fig. 2a, b) and a Western blot assay (Fig. 2c, d), more 20-kD protein (TrX alone) was produced after IPTG induction compared with no induction in the BL21(D3) *E. coli* cells transformed with the pET32a(+) vector (Fig. 2a, c). Similarly, IPTG promoted the expression of a protein of approximately 42 kD in the *E. coli* cells transformed with the pET32a(+)-CsHis vector (Fig. 2b, d). The observed molecular size showed good agreement with the size predicted from sequence data of the recombinant plasmid pET32a(+)-CsHis (CsHis 22.5 kD + TrX-tag 18.8 kD). The protein was therefore considered to be recombinant CsHis, implying that the molecular size of the CsHis protein is approximately 22.5 kD.

Expression of *CsHis* induced by abiotic stress

To investigate whether the expression of *CsHis* is induced by abiotic stress, the expression levels of *CsHis* were

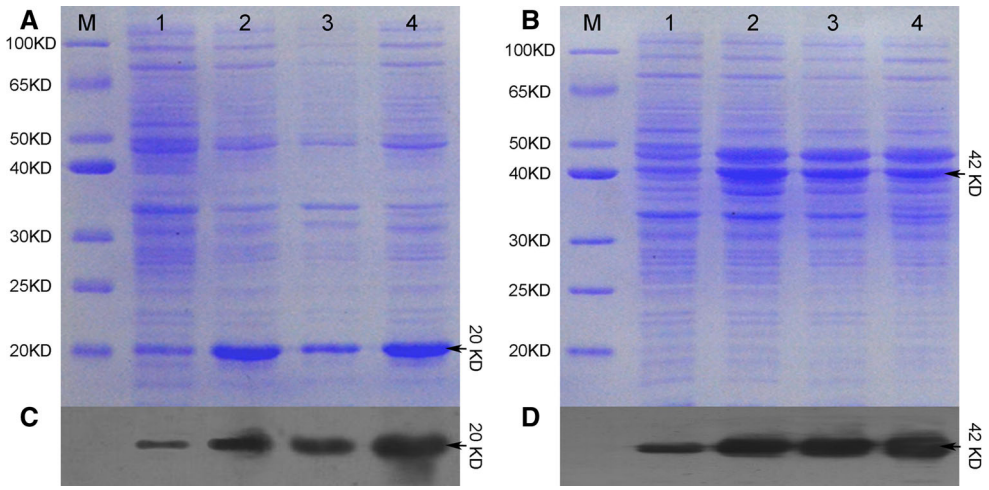

Fig. 2 SDS–PAGE analysis and Western blot detection of the CsHis protein. Protein expression levels of pET32a(+) (**a**) and pET32a(+)-CsHis (**b**) in BL21(DE3) *E. coli* cells were analyzed by SDS–PAGE. Western blot detection of TrX alone (**c**) and the TrX::CsHis fusion (**d**). *M* Protein maker, *1* un-induced, *2* total protein was induced by 0.2 mM IPTG at 37 °C, *3* precipitate after induction by 0.2-mM IPTG at 37 °C, *4* supernatant after induction by 0.2 mM IPTG at 37 °C. Proteins of TrX alone (approximately 20 kD) and the TrX::CsHis fusion (approximately 42 kD) are indicated by *black arrows*

examined by qRT-PCR under various abiotic stress treatments. As shown in Fig. 3a, the expression of *CsHis* increased gradually and peaked at 12 h after low-temperature treatment; thereafter, it decreased significantly. Similarly, the expression of *CsHis* strongly increased from 4 to 12 h after ABA treatment and was then maintained at a steady level (Fig. 3c). Additionally, *CsHis* expression increased continuously during the treatments with NaCl, PEG 6000 or H_2O_2 (Fig. 3b, d, e). In brief, the expression of *CsHis* is induced by various abiotic stresses, implying that *CsHis* participates in various stress responses in *C. sinensis*.

Obtaining transgenic tobacco plants that overexpress *CsHis*

The plant expression vector pCAMBIA2300-CsHis (Fig. S2A) was constructed and transformed into tobacco plants. As shown in Fig. S2B, a few kanamycin-resistant buds were induced from transgenic leaf discs after 30-day screening. These positive buds rooted and grew into robust transgenic plants in rooting medium supplemented with 50-mg L^{-1} kanamycin (Fig. S2C: His1-4), but the WT plants and the false-positive buds could not root and grow normally (Fig. S2C: WT, His5). Genomic PCR detection showed that the 624-bp product was detected in the His1, His2, His3 and His4 plants, but not in the His5 and WT plants (Fig. S2D). Additionally, green fluorescence was observed in the His1, His2, His3 and His4 plants but not in the His5 and WT plants (data not shown). Similarly, RT-PCR analysis showed that obvious bands were detected in the His1, His2, His3 and His4 plants, but no bands were detected in the His5 and WT plants (Fig. 4), implying that *CsHis* was expressed in the His1, His2, His3 and His4 plants. Furthermore, the expression levels of *CsHis* in the His2 and His4 plants were higher than those in the His1 and His3 plants (Fig. 4). Therefore, His2 and His4 of the transgenic tobacco plants were used for subsequent study.

Ultrastructural detection of nuclei in transgenic tobacco plants

Ultrastructure detection showed that the nuclei of WT plant cells appeared to have typical morphological shape, namely, the chromatin was dispersed and filled the nuclei (Fig. 5a, d). In contrast, the chromatin was condensed to a certain extent in the cells of the His2 (Fig. 5b, e) and His4 (Fig. 5c, f) plants, and the altered chromatin did not resemble the condensed and marginalized chromatin that sometimes appears in apoptotic tobacco cells (Fig. S3). These results confirmed that the CsHis protein is involved in the assembly and compression of high-order chromatin.

Overexpression of *CsHis* in tobacco improved tolerance to abiotic stresses

Leaf disc assay

As shown in Fig. 6, larger areas of damage (Fig. 6a) and lower chlorophyll content (Fig. 6b) were observed in the leaf discs of the WT tobacco plants after low-temperature treatment, while the leaf discs of the transgenic tobacco plants only suffered slight damage and remained green. Similarly, the leaf disc edges of the WT plants showed more

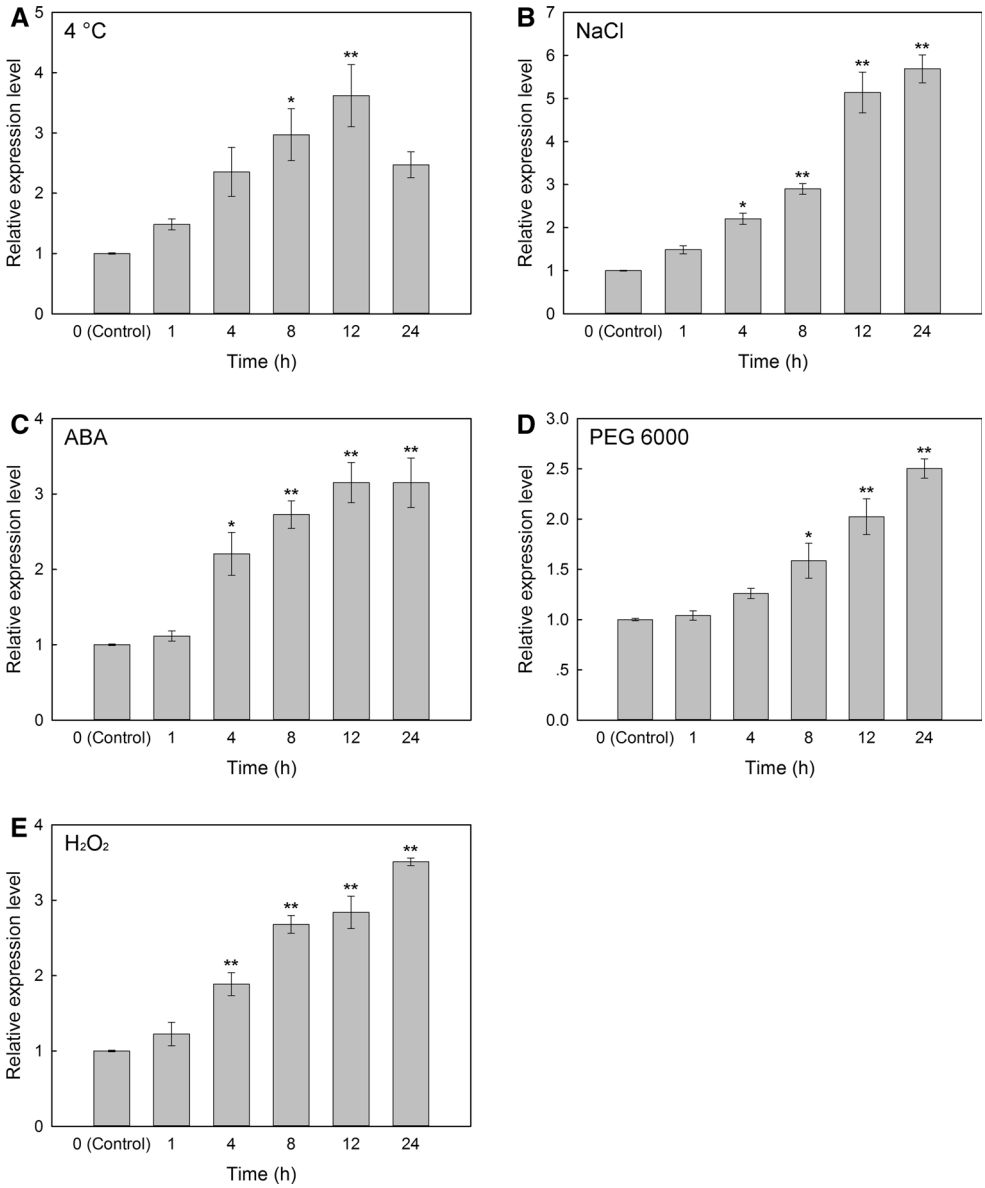

Fig. 3 Expression levels of *CsHis* in *C. sinensis* upon treatment with various abiotic stresses were analyzed by qRT-PCR. **a** Low-temperature treatment (4 °C), **b** high-salinity stress (600-mM NaCl), **c** treatment with 200-μM ABA, **d** drought stress (20 % PEG 6000), and **e** oxidative stress (100-mM H_2O_2) results are shown. Each value represents the mean of three independent biological replicates, and *vertical bars* indicate the SD. $*P < 0.05$ and $**P < 0.01$ indicate significant differences between treatments and the untreated control (Tukey's test)

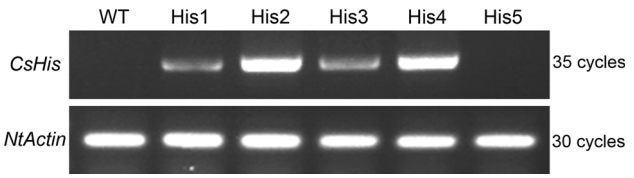

Fig. 4 *CsHis* expression levels in transgenic tobacco plants by RT-PCR. In His2 and His4 plants, the expression levels of *CsHis* were higher than those in His1 and His3 plants. No bands representing *CsHis* expression were detected in His5 or WT plants. *Actin* from tobacco (Genbank No. AB158612) was used as a quantitative control

severe bleaching and dying (Fig. 6a) and lower chlorophyll content (Fig. 6b) than the transgenic plants after NaCl or H_2O_2 treatment. Additionally, the leaf discs exhibited chlorosis and senescence upon ABA or PEG 6000 treatment, and this phenomenon was more obvious in the WT plants than in the transgenic plants (Fig. 6a), and the chlorophyll content of the transgenic plants was higher than that of the WT plants as well (Fig. 6b). These results showed that the leaf discs of the WT plants exhibited more severe damage, chlorosis and senescence (Fig. 6a) and lower chlorophyll content (Fig. 6b) compared with the leaf discs from the His2 and His4 plants, indicating the higher tolerance of the transgenic tobacco plants to abiotic stresses.

Analysis of plant tolerance to abiotic stress

As shown in Fig. 7, the transgenic tobacco plants showed greater tolerance compared with the WT tobacco plants

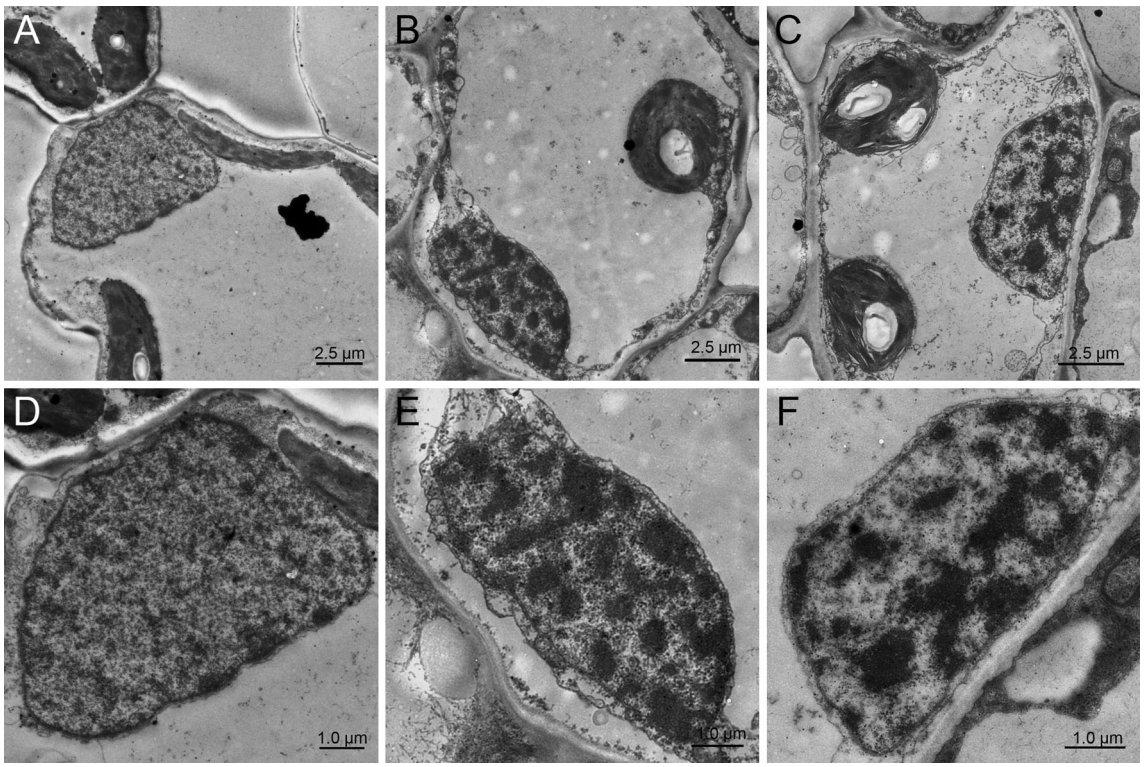

Fig. 5 Ultrastructural morphology of the nuclei in transgenic tobacco plants detected by TEM. Chromatin in WT tobacco cells is dispersed, filling the entire nucleus (**a**, **d**). In the nuclei of His2 (**b**, **e**) and His4 (**c**, **f**) cells, the chromatin was partially condensed

upon exposure to various abiotic stresses. For example, leaf wilting and senescence were reduced in the transgenic plants compared with the WT plants, and this difference was more obvious when the plants were treated with NaCl or H_2O_2. Additionally, the net photosynthetic rate (Pn) and stomatal conductance (Gs) were measured to determine the cause for the phenotypic differences observed above. The results showed that there was almost no difference in Pn between the transgenic (His2 and His4 plants) and WT plants under normal growth conditions (Fig. 8a), while Pn of both the transgenic and WT plants declined after various abiotic stresses. More interestingly, Pn values of the transgenic plants were significantly higher than that those in the corresponding WT plants (Fig. 8a). Moreover, the Gs response to abiotic stresses showed a similar pattern to that of Pn (Fig. 8b). We compared the maximum photochemical efficiency of PSII (Fv/Fm) in the dark-adapted state. As shown in Fig. 8c, d, various abiotic stresses resulted in significant decreases in Fv/Fm in both the WT and transgenic plants, but the Fv/Fm of the transgenic plants upon stress treatment was significantly higher than that of the corresponding WT plants. These results showed that the overexpression of *CsHis* could improve tolerance to abiotic stresses and maintain photosynthetic efficiency in transgenic tobacco plants.

Discussion

H1 histone, a linker histone, is a structural protein of chromatin in both plant and animal cells (Ascenzi and Gantt 1999; Breneman et al. 1993). Previous studies showed that H1 histone predominantly localizes to the nucleus in plant cells (Tanaka et al. 1999; Wang et al. 2012a). In our investigation, we also found that the CsHis protein localizes to the nucleus in onion epidermal cells and transgenic tobacco cells (Fig. 1), revealing that the CsHis protein is a nucleus-localized protein in *C. sinensis*. Moreover, prokaryotic expression analysis revealed that the molecular size of CsHis protein is approximately 22.5 kD, which resembles the findings of Wei and O'Connell (1996) and Ascenzi and Gantt (1997).

Previously, H1 histone was considered as only a structural protein of chromatin in plant cells (Laybourn and Kadonaga 1991; Prymakowska-Bosak et al. 1996), but increasing evidence has indicated that H1 histone plays a key role in responding to various stresses in plants (Jerzmanowski et al. 2000; Przewloka et al. 2002). Recent studies have shown that *H1 histone* can be induced by drought and ABA treatments in tomato (Scippa et al. 2000; Wei and O'Connell 1996) and *Arabidopsis* (Ascenzi and Gantt 1997). Similarly, our data revealed that the

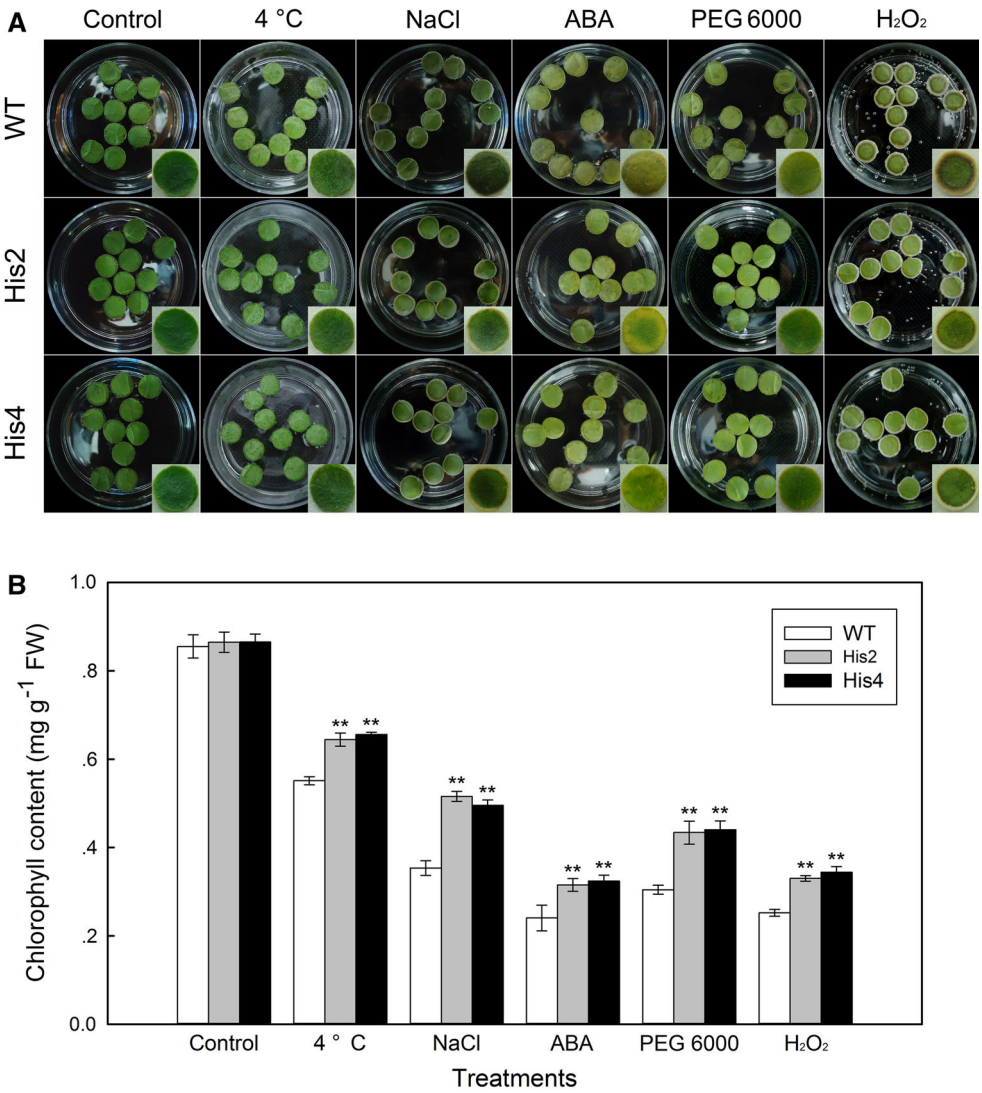

Fig. 6 Effects of various abiotic stresses on the phenotypes and chlorophyll contents of leaf discs from transgenic and WT tobacco plants. **a** Phenotypic differences of the leaf discs between transgenic (His2 and His4) and WT plants after various treatments. For all panels, insets highlight phenotypic differences of leaf discs after various treatments. **b** Chlorophyll contents (mg g^{-1} fresh weight, FW) of leaf discs from His2 and His4 of transgenic and WT plants were detected by the spectrophotometric method after 5 days of treatment with various abiotic stresses. Values are presented as mean ± SD from three independent experiments. $*P < 0.05$ and $**P < 0.01$ represent significant differences compared with WT plants (Tukey's test)

expression of *CsHis* is induced by different abiotic stresses, including low-temperature, high-salinity, ABA, drought and oxidative stress. Interestingly, it has been reported that cold stress upregulates the expression of *H1 histone* in Arabidopsis (Kreps et al. 2002) and downregulates it in rice (Neilson et al. 2011). Our results are consistent with the results of Kreps et al. (2002) but disagree with the results of Neilson et al. (2011), implying that *H1 histone* may affect the response to cold stress differently in different plant species. According to these results, it is reasonable to speculate that CsHis participates in the response to abiotic stress in *C. sinensis*.

To further study the roles of CsHis in abiotic stress responses, CsHis was overexpressed in tobacco plants, and two high-expression lines were obtained in the present study. The results indicated that chromatin was partially condensed in the cells of CsHis-overexpressing tobacco plants (His2 and His4 plants), which is similar to the observations of Prymakowska-Bosak et al. (1996), who reported that overexpressing H1 histone of *Arabidopsis* in tobacco resulted in serious chromatin conglomerations. This finding confirms that CsHis is involved in the assembly and compression of high-order chromatin structures. Therefore, we suspect that excessive CsHis protein increases the degree of chromatin compression, which induces chromatin condensation in transgenic tobacco plant cells. Furthermore, Prymakowska-Bosak et al. (1996) reported that dramatic changes in chromatin structure accompanied phenotypic changes and abnormal growth such as short stature, leaf variations, flowering abnormalities and abortion. However, it is interesting that the vegetative and reproductive growth in the transgenic tobacco plants was similar to that of the WT plants in our study, indicating that the chromatin condensation that resulted from *CsHis* overexpression barely affected the growth and development of the transgenic tobacco plants (Fig. S4).

Fig. 7 Phenotypic differences between transgenic (His2 and His4) and WT tobacco plants under abiotic stress

According to Prymakowska-Bosak et al. (1999), variants of H1 Histone in tobacco plants include H1A, H1B, H1C, H1D, H1E and H1F. H1A and H1B deletions induce stamen shortening and pollen deformity in tobacco (Prymakowska-Bosak et al. 1999; Przewloka et al. 2002), and leaf-type changes, the disappearance of apical dominance, flowering delay and flower abnormalities are observed in *Arabidopsis* (Wierzbicki and Jerzmanowski 2005), indicating that H1A and H1B are essential for normal growth and development in plants. Additionally, H1C and H1D are significantly induced by drought, ABA, salinity and cold stresses (Jerzmanowski et al. 2000; Przewloka et al. 2002; Wei and O'Connell 1996), suggesting that these histones play important roles in abiotic stress tolerance rather than the maintenance of normal growth and development (Przewloka et al. 2002). In the present study, phylogenetic analysis of plant H1 histones revealed that CsHis belongs to the H1C and H1D variants of H1 histone (Fig. S5), which is consistent with the above phenomena, i.e., overexpressing CsHis has almost no effect on plant morphology but only affects the response to abiotic stresses.

It is well known that abiotic stress affects the normal physiological processes of plants, such as photosynthesis, respiration and transpiration. Therefore, physiological changes are important indicators of plant stress tolerance. However, there are few available reports on how H1 histone affects plant physiological processes under abiotic stresses. Our data indicate that CsHis alleviates the damage to and senescence of leaf discs from transgenic tobacco plants under various abiotic stresses, including low-temperature, high-salinity, ABA, drought and oxidative stress (Fig. 7). Meanwhile, compared with the WT tobacco plants, the CsHis-overexpressing tobacco plants exhibited greater tolerance to abiotic stresses; for example, leaf wilting and senescence were reduced in the transgenic plants compared with the WT plants. Therefore, this result confirms that CsHis plays an important role in improving stress tolerance in plants. It has been reported that stresses decrease photosynthesis and chlorophyll fluorescence parameters such as Pn, Gs and Fv/Fm (Gorbe and Calatayud 2012). Fv/Fm was almost constant in different plant species under non-stress conditions with a value between 0.80 and 0.86 (Scarascia-Mugnozza et al. 1996). Fv/Fm has commonly been used to evaluate the running status of PSII and the resistance to environmental stress in plants (Abdeshahian et al. 2010; Gao et al. 2012). In the present

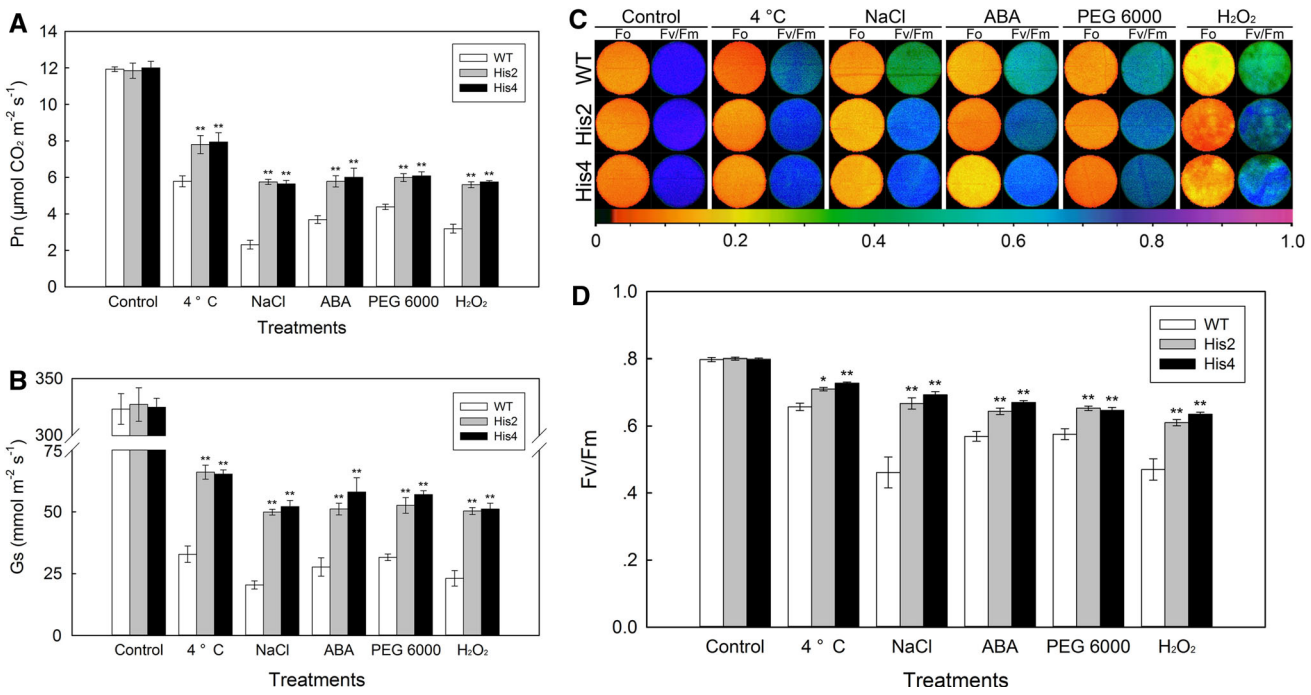

Fig. 8 Effects of various abiotic stresses on photosynthesis and chlorophyll fluorescence in leaves of transgenic (His2 and His4) and WT tobacco plants. **a** Net photosynthetic rate (Pn). **b** Stomatal conductance to CO_2 (Gs). **c** Images of Fv/Fm (*right*) after different treatments; F_0 (*left*) was used as the control. The pseudocolored bar depicted at the bottom of the image ranges from 0 (*black*) to 1.0 (*purple*). Similar results were obtained from three independent experiments, and one representative series of leaf discs is shown. **d** Average values of Fv/Fm. Pn and Gs values represent mean ± SD from five different leaves ($n = 5$), and Fv/Fm values are presented as mean ± SD from three independent experiments ($n = 3$). * $P < 0.05$ and ** $P < 0.01$ show significant differences compared with WT plants (Tukey's test) (color figure online)

study, Pn and Gs were higher in the transgenic tobacco plants than in the WT plants after various abiotic stress treatments. Similarly, the Fv/Fm values of the transgenic tobacco plants were significantly higher than those of the WT tobacco plants after stress treatments. These findings suggest that CsHis might contribute to the maintenance of a higher photochemical conversion efficiency of PSII and a higher electron transport capacity under various abiotic stresses (Osmond and Grace 1995). Taken together, our data reveal that CsHis improves tolerance to various abiotic stresses in the transgenic tobacco plants, possibly through the maintenance of photosynthetic efficiency.

In summary, the expression levels of *CsHis* detected by qRT-PCR showed that *CsHis* is a stress-induced gene, suggesting that CsHis participates in the responses to various abiotic stresses including low-temperature, high-salinity, ABA, drought and oxidative stress in *C. sinensis*. The overexpression of *CsHis* in tobacco promoted chromatin condensation, but barely affected the normal growth and development of the transgenic tobacco plants. Phylogenetic analysis of plant H1 histones showed that CsHis belongs to the stress-induced H1C and H1D variants, which explains the lack of an effect on normal growth and development. Moreover, direct evidence indicates that CsHis improves the tolerance to various abiotic stresses in the transgenic tobacco plants, possibly through the maintenance of photosynthetic efficiency of plants, which would be highly valuable for further research into the biological functions of H1 histone and for enhancing plant tolerance to environmental stress.

Acknowledgments This work was supported by National Natural Science Foundation of China (No. 31370014) and the earmarked fund for Modern Agro-industry Technology Research System (CARS-23).

Conflict of interest The authors declare that they have no conflict of interest.

References

Abdeshahian M, Nabipour M, Meskarbashee M (2010) Chlorophyll fluorescence as criterion for the diagnosis salt stress in wheat (*Triticum aestivum*) plants. Int J Chem Biol Eng 4:184–186

Alsaadawi IS, Al-Hadithy SM, Arif MB (1986) Effects of three phenolic acids on chlorophyll content and ions uptake in cowpea seedlings. J Chem Ecol 12:221–227

Ascenzi R, Gantt JS (1997) A drought-stress-inducible histone gene in *Arabidopsis thaliana* is a member of a distinct class of plant linker histone variants. Plant Mol Biol 34:629–641

Ascenzi R, Gantt JS (1999) Subnuclear distribution of the entire complement of linker histone variants in *Arabidopsis thaliana*. Chromosoma 108:345–355

Basak M, Sharma M, Chakraborty U (2001) Biochemical responses of *Camellia sinensis* (L.) O. Kuntze to heavy metal stress. J Environ Biol 22:37–41

Breneman JW, Yau P, Teplitz RL, Bradbury EM (1993) A light microscope study of linker histone distribution in rat metaphase chromosomes and interphase nuclei. Exp Cell Res 206:16–26

Das A, Das S, Mondal TK (2012) Identification of differentially expressed gene profiles in young roots of tea [*Camellia sinensis* (L.) O. Kuntze] subjected to drought stress using suppression subtractive hybridization. Plant Mol Biol Rep 30:1088–1101

Fang WP, Zhang Y, Zhou L, Wang WD, Li XH (2013) Isolation and characterization of *Histone1* gene and its promoter from tea plant (*Camellia sinensis*). Mol Biol Rep 40:3641–3648

Fu GQ, Xu S, Xie YJ, Han B, Nie L, Shen WB, Wang R (2011) Molecular cloning, characterization, and expression of an alfalfa (*Medicago sativa* L.) heme oxygenase-1 gene, *MsHO1*, which is pro-oxidants-regulated. Plant Physiol Bioch 49:792–799

Gao YS, Huang WF, Zhu LY, Chen JS (2012) Effects of $LaCl_3$ on the growth and photosynthetic characteristics of Fny-infected tobacco seedlings. J Rare Earth 30:725–730

Gorbe E, Calatayud A (2012) Applications of chlorophyll fluorescence imaging technique in horticultural research: a review. Sci Hortic-Amsterdam 138:24–35

Huang WM, Xing W, Li DH, Liu YD (2009) Morphological and ultrastructural changes in tobacco BY-2 cells exposed to microcystin-RR. Chemosphere 76:1006–1012

Jayawardene N, Riggs CD (1994) Molecular cloning, sequence analysis and differential expression of an intron-containing gene encoding tomato histone H1. Eur J Biochem 223:693–699

Jerzmanowski A, Przewłoka M, Grasser KD (2000) Linker histones and HMG1 proteins of higher plants. Plant Biol 2:586–597

Kornberg RD, Lorch Y (1999) Twenty-five years of the nucleosome, fundamental particle of the eukaryote chromosome. Cell 98:285–294

Kreps JA, Wu YJ, Chang HS, Zhu T, Wang X, Harper JF (2002) Transcriptome changes for *Arabidopsis* in response to salt, osmotic, and cold stress. Plant Physiol 130:2129–2141

Laybourn PJ, Kadonaga JT (1991) Role of nucleosomal cores and histone H1 in regulation of transcription by RNA polymerase II. Science 254:238–245

Li XW, Feng ZG, Yang HM, Zhu XP, Liu J, Yuan HY (2010) A novel cold-regulated gene from *Camellia sinensis*, *CsCOR1*, enhances salt-and dehydration-tolerance in tobacco. Biochem Biophys Res Co 394:354–359

Li L, Zhang C, Xu D, Schläppi M, Xu ZQ (2012) Expression of recombinant EARLI1, a hybrid proline-rich protein of *Arabidopsis*, in *Escherichia coli* and its inhibition effect to the growth of fungal pathogens and *Saccharomyces cerevisiae*. Gene 506:50–61

Liu W, An HM, Yang M (2013) Overexpression of *Rosa roxburghii* l-galactono-1, 4-lactone dehydrogenase in tobacco plant enhances ascorbate accumulation and abiotic stress tolerance. Acta Physiol Plant 35:1617–1624

Livak KJ, Schmittgen TD (2001) Analysis of relative gene expression data using real-time quantitative PCR and the $2^{-\Delta\Delta CT}$ method. Methods 25:402–408

Neilson KA, Mariani M, Haynes PA (2011) Quantitative proteomic analysis of cold-responsive proteins in rice. Proteomics 11:1696–1706

Osmond CB, Grace SC (1995) Perspectives on photoinhibition and photorespiration in the field: quintessential inefficiencies of the light and dark reactions of photosynthesis? J Exp Bot 46:1351–1362

Prymakowska-Bosak M, Przewłoka MR, Iwkiewicz J, Egierszdorff S, Kuraś M, Chaubet N, Gigot C, Spiker S, Jerzmanowski A (1996) Histone H1 overexpressed to high level in tobacco affects certain developmental programs but has limited effect on basal cellular functions. Proc Natl Acad Sci USA 93:10250–10255

Prymakowska-Bosak M, Przewloka MR, Ślusarczyk J, Kuraś M, Lichota J, Kiliańczyk B, Jerzmanowski A (1999) Linker histones play a role in male meiosis and the development of pollen grains in tobacco. Plant Cell 11:2317–2329

Przewloka MR, Wierzbicki AT, Ślusarczyk J, Kuraś M, Grasser KD, Stemmer C, Jerzmanowski A (2002) The "drought-inducible" histone H1s of tobacco play no role in male sterility linked to alterations in H1 variants. Planta 215:371–379

Raghuram N, Carrero G, Th'ng J, Hendzel MJ (2009) Molecular dynamics of histone H1. Biochem Cell Biol 87:189–206

Razafimahatratra P, Chaubet N, Philipps G, Gigot C (1991) Nucleotide sequence and expression of a maize H1 histone cDNA. Nucleic Acids Res 19:1491–1496

Sambrook J, Russell DW (2001) Molecular cloning: a laboratory manual, 3rd edn. Cold Spring Harbor Laboratory Press, New York

Scarascia-Mugnozza G, Angelis PD, Matteucci G, Valentini R (1996) Long-term exposure to elevated $[CO_2]$ in a natural *Quercus ilex* L. community: net photosynthesis and photochemical efficiency of PSII at different levels of water stress. Plant Cell Environ 19:643–654

Scippa GS, Griffiths A, Chiatante D, Bray EA (2000) The H1 histone variant of tomato, H1-S, is targeted to the nucleus and accumulates in chromatin in response to water-deficit stress. Planta 211:173–181

Shen XT, Gorovsky MA (1996) Linker histone H1 regulates specific gene expression but not global transcription in vivo. Cell 86:475–483

Szekeres M, Haizel T, Adam E, Nagy F (1995) Molecular characterization and expression of a tobacco histone H1 cDNA. Plant Mol Biol 27:597–605

Tanaka I, Akahori Y, Gomi K, Suzuki T, Ueda K (1999) A novel histone variant localized in nucleoli of higher plant cells. Chromosoma 108:190–199

Trivedi I, Ranjan A, Sharma YK, Sawant S (2012) The histone H1 variant accumulates in response to water stress in the drought tolerant genotype of *Gossypium herbaceum* L. Protein J 31:477–486

Voelker T, Sturm A, Chrispeels MJ (1987) Differences in expression between two seed lectin alleles obtained from normal and lectin-deficient beans are maintained in transgenic tobacco. EMBO J 6:3571–3577

Wan Q, Xu RK, Li XH (2012) Proton release by tea plant (*Camellia sinensis* L.) roots as affected by nutrient solution concentration and pH. Plant Soil Environ 58(9):429–434

Wang JN, Kuang JF, Shan W, Chen J, Xie H, Lu WJ, Chen JW, Chen JY (2012a) Expression profiles of a banana fruit linker histone H1 gene *MaHIS1* and its interaction with a WRKY transcription factor. Plant Cell Rep 31:1485–1494

Wang YH, Li XC, Zhu-Ge Q, Jiang X, Wang WD, Fang WP, Chen X, Li XH (2012b) Nitric oxide participates in cold-inhibited *Camellia sinensis* pollen germination and tube growth partly via cGMP in vitro. PloS One 7(12):e52436

Wei T, O'Connell MA (1996) Structure and characterization of a putative drought-inducible H1 histone gene. Plant Mol Biol 30:255–268

Widom J (1998) Chromatin structure: linking structure to function with histone H1. Curr Biol 8:R788–R791

Wierzbicki AT, Jerzmanowski A (2005) Suppression of histone H1 genes in *Arabidopsis* results in heritable developmental defects

and stochastic changes in DNA methylation. Genetics 169:997–1008
Wolffe AP, Khochbin S, Dimitrov S (1997) What do linker histones do in chromatin? BioEssays 19:249–255
Yang P, Katsura M, Nakayama T, Mikami K, Iwabuchi M (1991) Molecular cloning and nucleotide sequences of cDNAs for histone H1 and H2B variants from wheat. Nucleic Acids Res 19:5077